Geometric morphometric analysis of the crown morphology of the lower first premolar of hominins, with special attention to Pleistocene *Homo*

Aida Gómez-Robles [a,*], María Martinón-Torres [a], José María Bermúdez de Castro [a], Leyre Prado [a], Susana Sarmiento [a], Juan Luis Arsuaga [b]

[a] Centro Nacional de Investigación sobre Evolución Humana (CENIEH), Avda. de la Paz, 28, 09006, Burgos, Spain
[b] Centro de Evolución y Comportamiento Humanos. C/Sinesio Delgado, 4, pabellón 14, 28029 Madrid, Spain

Keywords:
Middle Pleistocene European populations
Dental anthropology
Procrustes superimposition
Allometry

A B S T R A C T

This article is the third of a series that explores hominin dental crown morphology by means of geometric morphometrics. After the analysis of the lower second premolar and the upper first molar crown shapes, we apply the same technique to lower first premolar morphology. Our results show a clear distinction between the morphology seen in earlier hominin taxa such as *Australopithecus* and African early *Homo*, as well as Asian *H. erectus*, and more recent groups such as European *H. heidelbergensis, H. neanderthalensis*, and *H. sapiens*. The morphology of the earlier hominins includes an asymmetrical outline, a conspicuous talonid, and an occlusal polygon that tends to be large. The morphology of the recent hominins includes a symmetrical outline and a reduced or absent talonid. Within this later group, premolars belonging to *H. heidelbergensis* and *H. neanderthalensis* tend to possess a small and mesiolingually-displaced occlusal polygon, whereas *H. sapiens* specimens usually present expanded and centered occlusal polygons in an almost circular outline. The morphological differences among *Paranthropus, Australopithecus*, and African early *Homo* as studied here are small and evolutionarily less significant compared to the differences between the earlier and later homin taxa. In contrast to the lower second premolar and the upper first molar crown, the inclusion of a larger hominin sample of lower first premolars reveals a large allometric component.

Introduction

Recent publications have addressed the dental morphological differences among fossil hominins (Bailey, 2004; Bailey and Lynch, 2005; Martinón-Torres et al., 2006; Gómez-Robles et al., 2007), continuing a tradition that began with the examination of the occlusal morphology of earlier African Pliocene and Pleistocene hominin taxa (Wood and Abbot, 1983; Wood et al., 1983; Wood and Uytterschaut, 1987; Wood et al., 1988; Wood and Engleman, 1988). Other important contributions on hominin dental crown morphology include, among others, Tobias (1991), Irish (1998); Bermúdez de Castro et al. (1999); Lockwood et al. (2000); White et al. (2000); Irish and Guatelli-Steinberg (2003); Hlusko (2004) and Moggi-Cecchi et al. (2005), but most of these have not focused on the study of a single type of tooth. Our research group has previously used geometric morphometric techniques to examine the morphological variability of the hominin lower second premolar (P_4) and upper first molar (M^1) (Martinón-Torres et al., 2006; Gómez-Robles et al., 2007, respectively). These studies paid special attention to middle and late Pleistocene populations, but Pliocene and early Pleistocene specimens from Africa, Asia, and Europe were included to assess the significance of the observed variation. The present study follows the research line of these previous studies, and is part of a study of the whole hominin dentition by means of geometric morphometric techniques.

The advantages of using dental remains in hominin phylogenetic studies have been discussed elsewhere (e.g., Turner, 1969; Irish, 1993, 1997, 1998; Bailey, 2000, 2002a; Irish and Guatelli-Steinberg, 2003; Martinón-Torres, 2006). Previous studies on P_4 crown morphology have shown differences among species (Wood and Uytterschaut, 1987; Bailey and Lynch, 2005; Martinón-Torres et al., 2006). Despite the large variation in the lower first premolar (P_3) of *H. sapiens* (Kraus and Furr, 1953; Biggerstaff, 1969; Scott and Turner, 1997), some authors have suggested that some premolar crown morphologies may be taxonomically distinctive (Coppens, 1977; Leonard and Hegmon, 1987; Wood and Uytterschaut, 1987; Suwa et al., 1996). These reports have mainly studied P_3 morphology in early hominin species (Leonard and Hegmon, 1987; Wood and Uytterschaut, 1987; Suwa et al., 1996), and in some higher primate species (Coppens, 1977), but a comprehensive comparative analysis

* Corresponding author.
E-mail address: aida.gomez@cenieh.es (A. Gómez-Robles).

of P_3 crown morphology that samples throughout the hominin fossil record has not been published. We analyze a sample that includes most of the hominin Pliocene and Pleistocene species known to date, including the Atapuerca-Sima de los Huesos (SH) dental sample, the largest and most representative sample from the European middle Pleistocene (Arsuaga et al., 1997), as well as the Atapuerca-Gran Dolina sample, which represents the only available hominin dental evidence from the European early Pleistocene to date. These data are compared with large samples of *H. neanderthalensis* and *H. sapiens*, as well as with smaller samples of *Australopithecus, Paranthropus*, and other *Homo* species, in order to ascertain the polarity of the observed morphologies.

Methods based on the incidence and relative expression of discrete traits, such as the Arizona State University Dental Anthropology System (ASUDAS) (Turner et al., 1991) have proven to be only moderately successful for comparing tooth crown variation within and among later fossil hominin species (Bailey, 2002b; Martinón-Torres, 2006). Recently, many dental studies based on image analysis of the occlusal morphology of fossil hominins (e.g., Bailey, 2004; Bailey and Lynch, 2005; Martinón-Torres et al., 2006; Gómez-Robles et al., 2007; Moggi-Cecchi and Boccone, 2007), non-human extant primates (e.g., Bailey et al., 2004; Pilbrow, 2006; Hlusko et al., 2007), and recent modern human populations (e.g., Harris and Dinh, 2006; Perez et al., 2006; Bernal, 2007) have been published. Classical morphometric methods applied to image analyses (measurement of diameters and cusp areas) have demonstrated that African robust and non-robust groups differed in their P_3 morphology (Wood and Uytterschaut, 1987; Suwa et al., 1996). We have adopted geometric morphometric methods based on Procrustes superimposition techniques (Rohlf and Slice, 1990; Bookstein, 1991) to examine the morphological affinities among the hominin species included in this study. Wood and Uytterschaut (1987) used this methodology to assess the fissure pattern of some African Pliocene and Pleistocene premolars, but in the present study we use semilandmarks (Bookstein, 1997) to compare the variation in the outline and the internal morphology (understood as the disposition of the structures enclosed by the outline) of the occlusal surface of the P_3.

Our article aims to provide a comprehensive description of the changes in P_3 crown morphology during hominin evolution, paying special attention to the middle Pleistocene European populations and to the similarities and differences that they show with *H. sapiens* and *H. neanderthalensis*. We anticipate that the results of this study will contribute new and detailed morphological information to the ongoing debate about hominin phylogeny (e.g., Wood, 1992; Bermúdez de Castro et al., 1997; Foley and Lahr, 1997; Lahr and Foley, 1998; Rightmire, 1998; Stringer and Hublin, 1999; Wood and Collard, 1999; Stringer, 2002; Manzi, 2004; Dennell and Roebroecks, 2005; Martinón-Torres et al., 2007).

Materials and methods

Materials

A geometric morphometric analysis was performed on a sample of 106 hominin first premolars. The samples comprised the following number of specimens (Table 1): *A. anamensis* ($n=1$), *A. afarensis* ($n=7$), *A. africanus* ($n=5$), *Paranthropus sp.* ($n=3$), *H. habilis s. l.* ($n=5$), *H. ergaster* ($n=4$), *H. georgicus* ($n=2$), *H. erectus* ($n=10$), *H. antecessor* ($n=2$), *H. heidelbergensis* ($n=18$), *H. neanderthalensis* ($n=15$), and *H. sapiens* ($n=34$).

We used the same taxonomy as in Gómez-Robles et al. (2007). *Australopithecus* specimens were separated into three species: *A. anamensis, A. afarensis*, and *A. africanus*, whereas *Paranthropus* premolars were grouped together under the denomination *Paranthropus sp.* The *H. habilis s. l.* group included the African Pliocene specimens assigned to *H. habilis, H. rudolfensis*, and similar unassigned specimens. The taxon *H. erectus* (Dubois, 1894) was used for Asian premolars from Zhoukoudian, Sangiran, and Trinil. African specimens that some authors have attributed to *H. erectus s. l.* (Walker and Leakey, 1993) were designated as *H. ergaster* (Groves and Mázak, 1975), and we also included the African specimen from Rabat in this group. *H. georgicus* (Gabunia et al., 2002) and *H. antecessor* (Bermúdez de Castro et al., 1997) were analyzed separately on the basis of their general morphological distinction (Bermúdez de Castro et al., 1997; Gabunia et al., 2002), as well as their geographical and chronological separation from other groups. The term *H. heidelbergensis* (Schoetensack, 1908) was used for the European middle Pleistocene populations, such as Arago and Atapuerca-Sima de los Huesos samples. Finally, *H. neanderthalensis* comprised classic European Neandertals, while *H. sapiens* was represented by two modern human collections, one from the Institute of Anthropology of the University of Coimbra, dating from the Portuguese 19th–20th century ($n=12$, 6 males and 6 females), and the other held at the American Museum of Natural History in New York and coming from Heidenheim, Germany ($n=18$, 8 males and 10 females), together with some early anatomically modern humans and Upper Paleolithic *H. sapiens*.

Table 1
List of the specimens included in this analysis

Australopithecus anamensis ($n=1$)	KNM-KP29281 (cast)
Australopithecus afarensis ($n=7$)	A.L.198-23; A.L.207-13; A.L.266-1; A.L.288; A.L.333w-60; A.L.400-1a; LH4 (casts)
Australopithecus africanus ($n=5$)	MLD2; STS52; STW14; STW498; OMO75-148 (casts)
Paranthropus sp. ($n=3$)	KNM-ER 3230; OMO L427-7; TM1517 (casts)
Homo habilis s. l. ($n=5$)	KNM-ER 1802; OH 7; OH 13; OH 16; OMO 75i-1255 (casts)
Homo georgicus ($n=2$)	D211; D2735 (originals)
Homo ergaster ($n=4$)	KNM-ER 992; OH 22; KNM-WT 15000; Rabat (casts)
Homo erectus ($n=10$)	Zhoukoudian 20, 80, 35.77, G 1, K1.96 (casts) Sangiran 6, 7-25, 7-26, 7-69, Trinil (originals)
Homo antecessor ($n=2$)	ATD6-3; ATD6-96 (originals)
Homo heidelbergensis ($n=18$)	Arago 13; 71; 75 (originals) Sima de los Huesos: AT-2; AT-47; AT-4328; AT-4147; AT-3880; AT-2767; AT-809; AT-2768; AT-607; AT-2438; AT-3941; AT-148; AT-1466; AT-3243; AT-4100 (originals)
Homo neanderthalensis ($n=15$)	Krapina 25, 29, 33, 34, 111, 114, MbD, MbE, MbH; (casts) Hortus IV, VI; Guattari 3 (originals) Amud I; Le Moustier 1; Saint Cesaire (casts)
Homo sapiens ($n=34$)	Dolni Vestonice 13 (original) Grotte des Enfants 6; Qafzeh 9, 11 (casts) Modern humans from Portugal, Institute of Anthropology of the University of Coimbra ($n=18$) Modern humans from the American Museum of Natural History, New York, ($n=12$)

Taxonomical assignments of the isolated specimens from Zhoukoudian, Sangiran, and Shungura Formation follow Weidenreich (1937), Grine and Franzen (1994), and Suwa et al. (1996), respectively. These assignments, based mainly upon the morphology of the teeth (and also upon their geographical and chronological context), can be supported by our results. Relative warp analysis is independent of the taxonomy. CVA is dependent on the a priori assignment of the specimens, but the groups we have used in this analysis are ample enough to enclose the variability of those groups with isolated specimens.

Photographing the sample

We used standardized images of the occlusal surface of the premolars. Images were taken with a Nikon® D1H digital camera fitted with an AF Micro-Nikon 105 mm, f/2.8D. The camera was attached to a Kaiser Copy Stand Kit RS-1® with grid baseboard, column, and adjustable camera arm. For maximum depth of field, we used an aperture of f/32. The magnification ratio was adjusted

to 1:1, and a scale was placed parallel to and at the same distance from the lens as the occlusal plane.

In order to standardize the photographs, each tooth was positioned with the lens parallel to the cemento-enamel junction (CEJ) (Wood and Abbott, 1983; Wood and Uytterschaut, 1987; Bailey and Lynch, 2005; Martinón-Torres et al., 2006), as shown in Fig. 1. Isolated teeth were placed on modeling clay, and mandibles with premolars in situ were reoriented appropriately. The use of a standard orientation avoids methodological problems which may occur when 3D objects are projected onto a two dimensional surface (Gharaibeh, 2005). Nevertheless, the estimation of the standard plane can be difficult at times since the CEJ is not straight. Thus, subtle differences in the orientation of the reference plane might give different landmarks configurations as an artifactual effect of the CEJ morphology. As this effect has not been measured in previous papers of this series (Martinón-Torres et al., 2006; Gómez-Robles et al., 2007), an evaluation of the repeatability in the establishment of the reference plane is provided below.

When both antimeres were present, the right was chosen for study. However, in order to maximize the sample size, when the right one was not preserved or when the location of the landmarks was not clear, the left premolar was included for study. Left antimeres were mirror-imaged with Adobe Photoshop® before performing the analyses. Teeth with severe attritional wear and/or with uncertain location of one or more landmarks were not included in the study.

Geometric morphometric methods

Geometric morphometric methods based on Procrustes superimposition (Rohlf and Slice, 1990; Bookstein, 1991) are becoming one of the most used and powerful tools in morphological studies (Adams et al., 2004). Individual structures recovered as landmark

Fig. 1. Diagram showing the location of the plane through the CEJ that was placed parallel to the lens of the camera when photographing the premolars.

conformations are compared to the mean or consensus shape of the analyzed sample by means of Generalized Procrustes Analysis (GPA) (Rohlf and Slice, 1990; Dryden and Mardia, 1998). Landmark configurations are translated, scaled, and rotated until the distances among homologous landmarks are minimized according to least squares criteria. The square root of the sum of those squared distances is named Procrustes distance and is a measure of the morphological differences among biological structures. Such distance describes the entirety of the morphological differences among the studied structures (Zelditch et al., 2004).

Thin plate spline (TPS) provides a representation of the shape changes when one specimen is deformed into another one. Every shape change can be decomposed into a uniform component with equal effects on the complete structure, and a non uniform component with local effects on particular areas (Bookstein, 1991). The non uniform component requires bending energy, a measurement of the localization of the change of shape that provides a set of shape descriptors, the partial warps scores (Bookstein, 1989, 1991, 1996a; Rohlf, 1996). Principal components analysis (PCA) of the partial warps scores is the most common test in geometric morphometric studies and it is called relative warp analysis (Bookstein, 1991). This analysis reduces the total variability to a lower number of independent dimensions. Usually, the few first principal components capture the main patterns of morphological variation within the sample (Frieß, 2003). TpsRelw software (Rohlf, 1998a) was used to perform this analysis.

In addition to relative warp analysis, canonical variates analysis (CVA) was also used to discriminate among the different samples, since this analysis maximizes the inter-group variability relative to intra-group variability (Albrecht, 1980). An assignment test was performed after the CVA in order to determine the utility of P_3 shape in discriminating and determining the affinity of the groups established a priori (Nolte and Sheets, 2005). CVA requires that the number of specimens is at least as many as the number of variables (Hammer and Harper, 2006). Given the small sample size of some of the groups, a reduction of the number of variables included was necessary. The relative warp analysis previously carried out provided also a data reduction that allowed using a subset of the PCs instead of the original variables (Klingenberg, pers. comm.). CVA is able to be conducted in a reduced PCA space since the first PCs capture the most important aspects of the morphological change (Slice, pers. comm.).

Since the sample sizes of some fossil hominin taxa are too small (with the exception of the *H. heidelbergensis, H. neanderthalensis*, and *H. sapiens* samples), we merged some of the species into more inclusive samples to perform the CVA. Thus, the three *Australopithecus* species were pooled as *Australopithecus sp.*, and the *H. habilis* and *H. ergaster* samples were pooled as African *Homo*. The original Asian *H. erectus, H. heidelbergensis, H. neanderthalensis*, and *H. sapiens* samples were retained. The *Paranthropus sp., H. georgicus*, and *H. antecessor* specimens were not included in the CVA due to the difficulty of including them in any of the groups cited above. However, these specimens were later classified into one of the previous groups based on the discriminant function results of the analysis, and they were plotted in the CVA graph. Morphological variants corresponding to the extremes of the CVs were generated using TpsRegr (Rohlf, 1998b).

Landmarks and semilandmarks

Landmarks are biologically and geometrically homologous points among the studied specimens (Zelditch et al., 2004). The occlusal morphology of a P_3 crown consists of the two main cusps comprising the trigonid and a talonid. The median longitudinal fissure marks the boundary between the protoconid (buccal cusp) and the metaconid (lingual cusp). The distobuccal and distolingual

fovea/transverse fissures and their intersections with the buccal and lingual borders of the crown delimit the talonid area (Wood and Uytterschaut, 1987). The four landmarks within the occlusal outline (Fig. 2) were defined as follows (Biggerstaff, 1969; Wood and Uytterschaut, 1987):

Landmark 1: Tip of the buccal cusp or protoconid, determined by inspection.

Landmark 2: Posterior/distal fovea or the intersection of the median longitudinal fissure (also named central groove) with the distal fovea-fissures/transverse fissures (Biggerstaff, 1969; Wood and Uytterschaut, 1987). When the presence of a transverse crest erases the central groove, this landmark is located at the deepest point of the distal fovea.

Landmark 3: Tip of the lingual cusp or metaconid, determined by inspection.

Landmark 4: Anterior/mesial fovea or the intersection of the median longitudinal fissure (or central groove) with the mesial fovea fissures/transverse fissures (Biggerstaff, 1969; Wood and Uytterschaut, 1987). When the central groove is not present, this landmark is placed at the deepest point of the mesial fovea.

These landmarks were chosen because they can be accurately located even when some representative traits of the premolars are absent.

The use of semilandmarks was proposed by Bookstein to study the shape of structures that lack real landmarks, such as curves or outlines (Bookstein, 1996b, 1997; Bookstein et al., 1999). Whereas real landmarks contain shape information in all the directions of the coordinate system, semilandmarks are uninformative with respect to their exact location along a curve or outline (Bookstein, 1996b; Zelditch et al., 2004; Bastir et al., 2006), but sliding techniques avoid this limitation (Bookstein, 1996b, 1997; Bookstein et al., 2002; Gunz et al., 2005). The locations of the semilandmarks are allowed to slide along the curve to produce a new set of semilandmarks that either represents the smoothest possible mathematical deformation of the curve on the reference form to the corresponding curve on a particular specimen (minimum bending energy; Bookstein, 1996b, 1997; Sheets et al., 2004), or minimizes the Procrustes distance between the curve on the reference form and each individual in the sample (Sampson et al., 1996). The criterion employed in this analysis has been the minimization of the Procrustes distance.

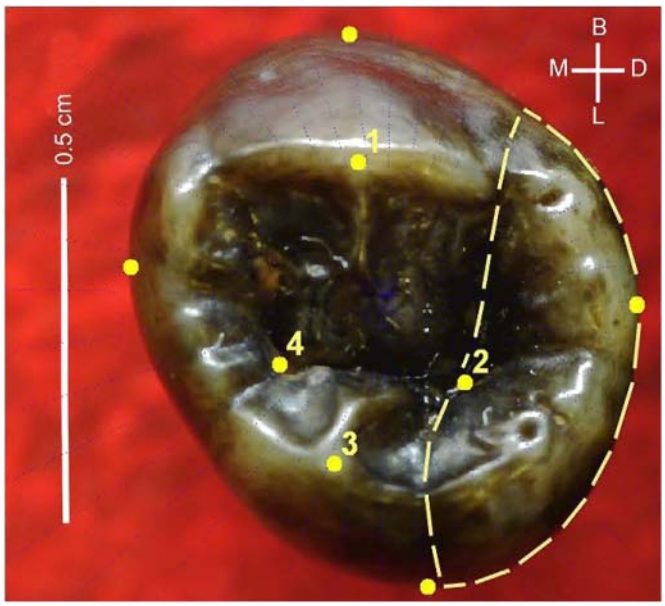

Fig. 2. Digitized image of a P_3 of *H. erectus* showing the four landmarks: 1) protoconid tip; 2) distal fovea; 3) metaconid tip; 4) mesial fovea. Four type III landmarks (the most buccal, the most distal, the most lingual, and the most mesial points of the crown) are also marked in the external contour of the tooth. These landmarks were employed to draw the forty semilandmarks, which would be later located at the intersection of the external outline and the fan lines (see text for explanation). Discontinuous line highlights the contour of the talonid. B: buccal; D: distal; L: lingual; M: mesial.

Landmarks were digitized by A. G.-R. The tips of the main cusps were visually located in the images while simultaneously examining the fossil or cast. The cusp tip was assumed to be in the center of the wear facet in those teeth where wear had removed it (Bailey, 2004; Martinón-Torres et al., 2006; Gómez-Robles et al., 2007). When mesial and/or distal borders of the teeth were affected by light interproximal wear, original borders were estimated by reference to overall crown shape and the buccolingual extent of the wear facets (see Wood and Uytterschaut, 1987; Bailey and Lynch, 2005, Martinón-Torres et al., 2006). Those premolars that were heavily worn were not included in the study. However, teeth with a moderate degree of wear were used since they have been demonstrated to provide consistent results when studied together with unworn teeth (Gómez-Robles et al., 2007).

Semilandmarks were drawn starting from four type III landmarks (extreme points in various dimensions which have at least one deficient coordinate; Bookstein, 1991) that were later removed. The chosen points were (Biggerstaff, 1969; Wood and Uytterschaut, 1987): the most buccal, the most distal, the most lingual, and the most mesial points of the crown. The gravity center of these four points was used as the central point to obtain forty equiangular fan lines (Fig. 2) with MakeFan6 software (Sheets, 2001). These points were used instead of the four studied landmarks to avoid an oversampling of the lingual half of those premolars with a predominantly lingual location of the landmarks. The points at which the fan lines intersected the premolar outline provided the initial location of the semilandmarks (before sliding). TpsDig (Rohlf, 1998c) was later used to digitize the landmarks and semilandmarks.

Allometry

Allometry is the study of any links between shape and overall size (Mosiman, 1970; Klingenberg, 1998), and several criteria have been proposed to study its incidence and influence over the shape of the organisms and their parts. We have focused on the study of the evolutionary allometry, analyzing the correlation between size and shape among taxonomically different populations, related either by ancestor-descendant relationships or as sister groups (Klingenberg, 1998; Bastir, 2004). For that reason, we have analyzed allometry in an inter-specific context. Although previous works have assumed that allometry has no influence on hominin dental morphology (Bailey and Lynch, 2005), the use of geometric morphometrics by means of a multivariate regression of partial warps and uniform component on centroid size, allows us to test that hypothesis. Centroid size, defined as the squared root of the summed squared distance between the centroid (or "gravity center" of the landmarks configuration) and each of the landmarks (Zelditch et al., 2004), was used as a proxy for overall size. Multivariate regression was accompanied by a permutation test ($n = 10000$) to evaluate the significance of the allometry using TpsRegr software (Rohlf, 1998b).

Measurement error

The evaluation of the measurement error was divided into two parts to independently assess the amount of error due to the location and digitizing of the landmarks and semilandmarks or due to the orientation of the tooth during photography. A subsample of five premolars (KNM-WT 15000, AT-1993 [left antimere not included in the analyses], AT-3243, Krapina114, and Krapina33) was

used to establish the error inherent in the method for data acquisition set out above. These premolars were randomly chosen among those that were available to rephotograph. Still, that subsample is representative of the original complete sample, given that both include casts, originals, and in situ and isolated premolars with different degrees of wear. To assess the error due to the digitizing process, the four landmarks and forty semilandmarks were digitized over five consecutive days on one photograph of each of the five teeth.

In order to measure the error due to the location of the reference plane when photographing the tooth, the five premolars were rephotographed over a period of five consecutive days, each time ensuring that the CEJ was parallel to the lens, as described above. Then, the landmarks and the four points employed to later locate the semilandmarks were visually placed in the same anatomical location by comparing the five images corresponding to each premolar. After that, the four landmarks and forty semilandmarks were digitized.

After a Procrustes superimposition of the described subsample, the Euclidean distances of each landmark to its respective centroid were computed using Tmorphgen6 software (Sheets, 2001), and landmark deviations were calculated relative to landmark means (Singleton, 2002). The scatter at each landmark for each individual was averaged in order to obtain a mean value of the error due to the orientation of the tooth when photographing it and due to the digitizing process. We are aware of the fact that the measurement of the dispersion at each landmark according to Singleton (2002) causes a slight underestimation when the dispersion is not collinear (von Cramon-Taubadel et al., 2007). Notwithstanding, this approach provides an estimate of the repeatability of our method of capturing the data.

The mean value of the scatter at each landmark relative to the landmark mean due to the digitizing process is 0.63% when semilandmarks are included and 2.24% if the error is calculated just for the landmarks. This level of error is within the range reported by similar studies (e.g., Singleton, 2002; Harvati, 2003). The Krapina 114 premolar had the lowest error, with a mean value of 0.45%, whereas AT-3243 had the highest, 0.89%. Since the error was calculated after the Procrustes superimposition, the sliding mechanism minimizes the error at semilandmarks, with values between 0.34% and 0.67%.

The amount of error due to the orientation of the premolars when they are photographed is higher. This error has a mean value of 1.23% with the inclusion of semilandmarks and 3.2% for the landmarks alone. The mean error values for each individual are similar and they range from 1.02% to 1.59%. Regarding landmark error, the apex of the protoconid has the highest error (4.33%) and the apex of the metaconid the lowest (2.08%). Again, the variability at semilandmarks is reduced by the sliding mechanism, with values between 0.17% and 2.43%.

The relatively high error at the location of the apex of the protoconid must be taken into account when interpreting the results of the analyses, especially those influenced by the location of the first landmark.

Results

The relative warps analysis shows that the two first principal components (PC1 and PC2) explain 55.3% of the total variability of the sample (43.2% and 12.1%, respectively; Table 2).

A negative score on the PC1 (Fig. 3) corresponds to asymmetrical premolars with a well-developed talonid that occupies the distal and distolingual portions of the occlusal surface. The presence of a conspicuous talonid causes the asymmetry of the premolars, which is related to the obliquity of the maximum bucolingual length relative to the mesiodistal axis. In teeth with a negative PC1 score, the occlusal polygon (the area enclosed by the straight lines connecting the four landmarks) is expanded (large in relation to the external contour of the tooth), and the apices of the protoconid and metaconid are displaced mesially. Teeth with a positive score on PC1 are almost symmetrical, with a smooth outline without any talonid protrusion, and a small and lingually-located occlusal polygon. The reduced occlusal polygon size is due to the relative migration of the protoconid tip toward the lingual face so the occlusal polygon is compressed and displaced to the lingual half of the premolar.

Table 2
Relative warps analysis showing the first ten principal components

No.	Singular value	% explained variance	% cumulative variance
1	0.48109	43.2	43.2
2	0.25493	12.1	55.3
3	0.23307	10.1	65.4
4	0.19198	6.9	72.3
5	0.15963	4.8	77.1
6	0.15801	4.7	81.8
7	0.14147	3.7	85.5
8	0.11805	2.6	88.1
9	0.10649	2.1	90.2
10	0.09102	1.5	91.7

A negative score on the PC2 is linked with a symmetrical P_3 crown, an oval outline, and a large and centrally-located occlusal polygon. A positive score on PC2 is characterized by asymmetrical premolars with conspicuous talonids but with small occlusal polygons.

The positive extremes of PC1 and PC2 are both linked with a centrally-located protoconid apex that results in a small and more lingually-located occlusal polygon, independent of the symmetry or asymmetry of the outline. Notwithstanding, the negative ends of PC1 and PC2 are correlated with relatively large occlusal polygons, in asymmetrical (PC1) and symmetrical (PC2) outlines.

The distribution of the specimens in the plot of the principal components (Fig. 3) shows strong separation between archaic (*Australopithecus, Paranthropus*, and early *Homo* species) and recent (*H. heidelbergensis, H. neanderthalensis*, and *H. sapiens*) hominin species. As we can see in Fig. 3, this differentiation can be emphasized by drawing an imaginary line in the morphospace, which separates almost completely the more recent *Homo* species from the more archaic ones.

All the *Australopithecus* specimens (except the *A. anamensis* premolar, one *A. africanus* [STW14], and one *A. afarensis* [A.L.288]) are located at the upper left quadrant of the plot, with negative values for PC1 and positive values for PC2. This is also the quadrant where other early hominin taxa are located (i.e., the three *Paranthropus* specimens, three out of five *H. habilis*, one *H. ergaster*, and both *H. antecessor* specimens). The *H. erectus* specimens, however, all plot with negative values for PC1, but they have either positive or negative values for PC2, with the Sangiran specimens tending to display positive scores, and the Zhoukoudian specimens mainly negative values, as is the case for the *H. georgicus* premolars. It is important to note that most of the African and Asian Pliocene and lower Pleistocene specimens have negative values on PC1, the only exceptions being the *A. anamensis* (KNM-KP29281) and one *H. ergaster* (KNM-ER 992) premolars.

Most *H. heidelbergensis* and *H. neanderthalensis* specimens have positive scores for PC1. The exceptions are the three specimens from Arago for *H. heidelbergensis*, and the Le Moustier and Krapina *H. neanderthalensis* specimens. The distribution patterns of those species are similar, except that the Sima de los Huesos sample shows more extreme positive values for PC1 and PC2, with a more marked reduction in size of the occlusal polygon, characteristic of this population.

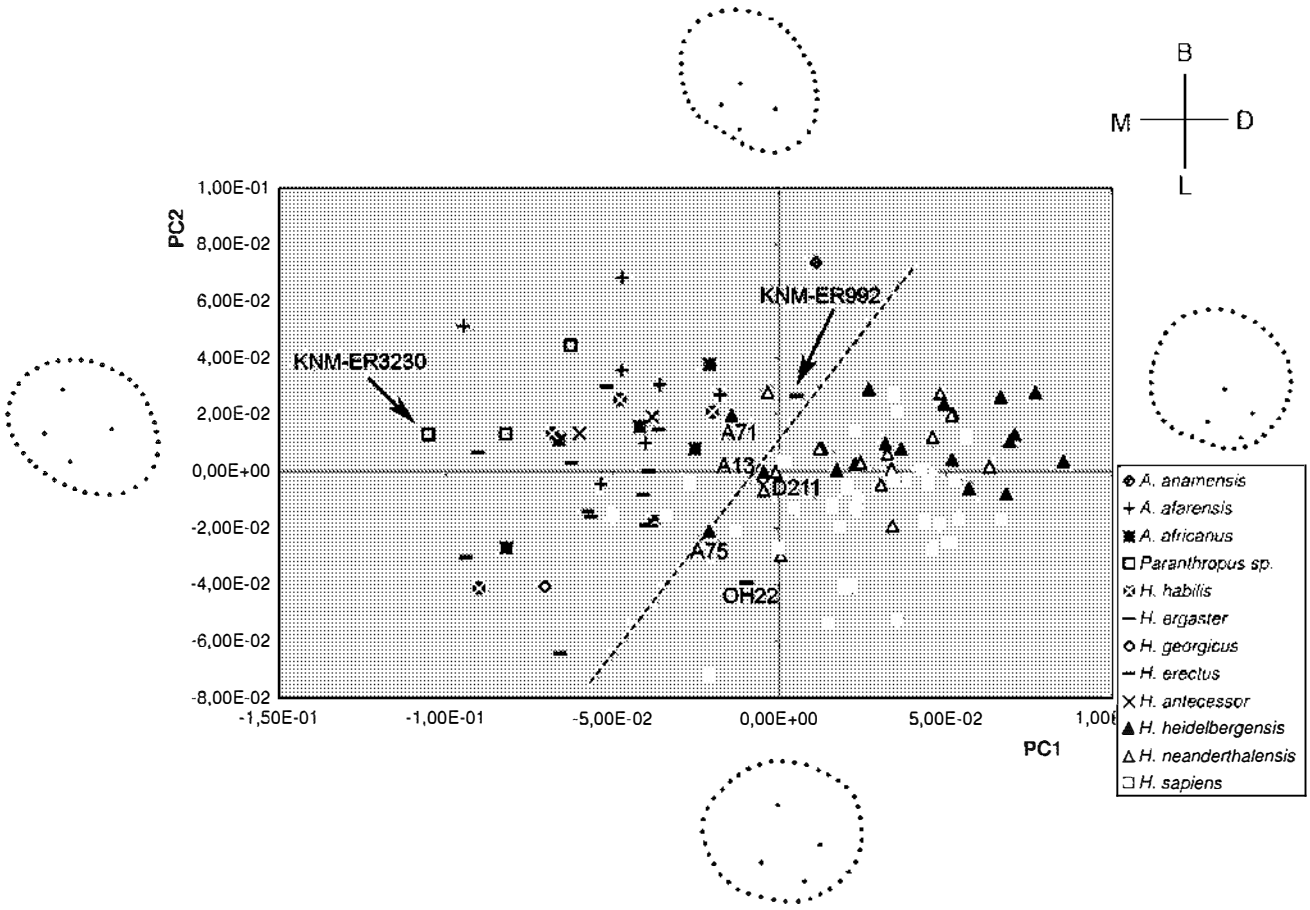

Fig. 3. Projection of individual P_3 crowns on PC1 and PC2. TPS-grids illustrate the morphological variation trends of the specimens along each principal component. These grids show how a TPS transformation of the mean shape into a theoretical specimen would look if its PC-score were at an extreme point on the one PC axis and zero at all other axes. The dotted line remarks the separation of early African and Asian specimens, characterized mainly by negative values for PC1, from more recent ones, which tend to show positive scores for that PC.

The *H. sapiens* sample predominantly plots in the lower right quadrant of the graph. Twenty-three out of 34 modern human first premolars plot with positive values for PC1 and negative values for PC2, without noticeable differences between the modern human samples from the AMNH and the University of Coimbra. Although some *H. sapiens* premolars are located in the upper right and lower left quadrants of the plot (Fig. 3), there is no *H. sapiens* specimen in the upper left quadrant, where the majority of the early African hominins cluster.

As canonical variates analysis (CVA) requires the number of cases of the smallest sample to be larger than the number of variables (Hammer and Harper, 2006), the nine first principal components (which account for the 90.04% of the variability of the sample) were chosen as variables for the CVA (since nine is the sample size of the smallest group, namely the African *Homo* sample). CVA works upon an assumption that variances across groups are homogeneous. As two of the groups included in this analysis (*Australopithecus sp.* and African *Homo*) contain morphologically diverse taxa, we determined whether the variance differs significantly between the a priori defined groups. Although the Levene statistic showed that the variances are homogeneous when the variables are considered separately (p-values between 0.084 and 0.95), the hypothesis of equal covariance matrices for those nine variables was rejected when using Box's M statistic ($p \leq 0.0001$). However, when the number of variables included in the CVA was reduced to the first five PCs, this resulted in the homogeneity of the covariance matrices ($p = 0.078$, Box's M) with only a small reduction in the percentage of variability of the sample included in the CVA (77.1% with five variables versus 90.2% with nine variables).

The CVA (Fig. 4) yielded similar results to the relative warps analysis (PCA). The CVA extracted five canonical variables (Table 3) of which the first two explain 93.6% of the variation (from the 77.1% of the total variation of the sample included in this analysis).

Specimens at the negative end of CV1 (Fig. 4) have asymmetrical morphologies with conspicuous talonids and large occlusal polygons, whereas specimens at the positive end show almost circular and symmetrical outlines. This difference is due to a reduction of the talonid and to the relative migration of the protoconid tip to the center of the tooth. Thus, the positive end of CV1 corresponds to P_3s with rounded occlusal outlines and small and lingually-located occlusal polygon. A P_3 with an oval outline and relatively large occlusal polygon would plot at the negative end of CV2, with the protoconid apex and the anterior fovea peripherally located regarding to their location at the positive end of CV2. Positive scores on CV2 correspond to a slightly asymmetrical P_3s, with a reduced talonid that mainly occupies the distolingual portion of the crown and with a compressed occlusal polygon located mesio-lingually. P_3s with positive scores for CV2 have a uniform and slightly convex distal outline, whereas the mesial side tends to be more concave, with an inflexion at the level of the mesio-lingual groove when it intersects the external outline.

In general, the distribution of the premolars on the CVA plot coincides with the PCA distribution by showing a clear distinction between the early hominins (*Australopithecus sp.*, African *Homo*,

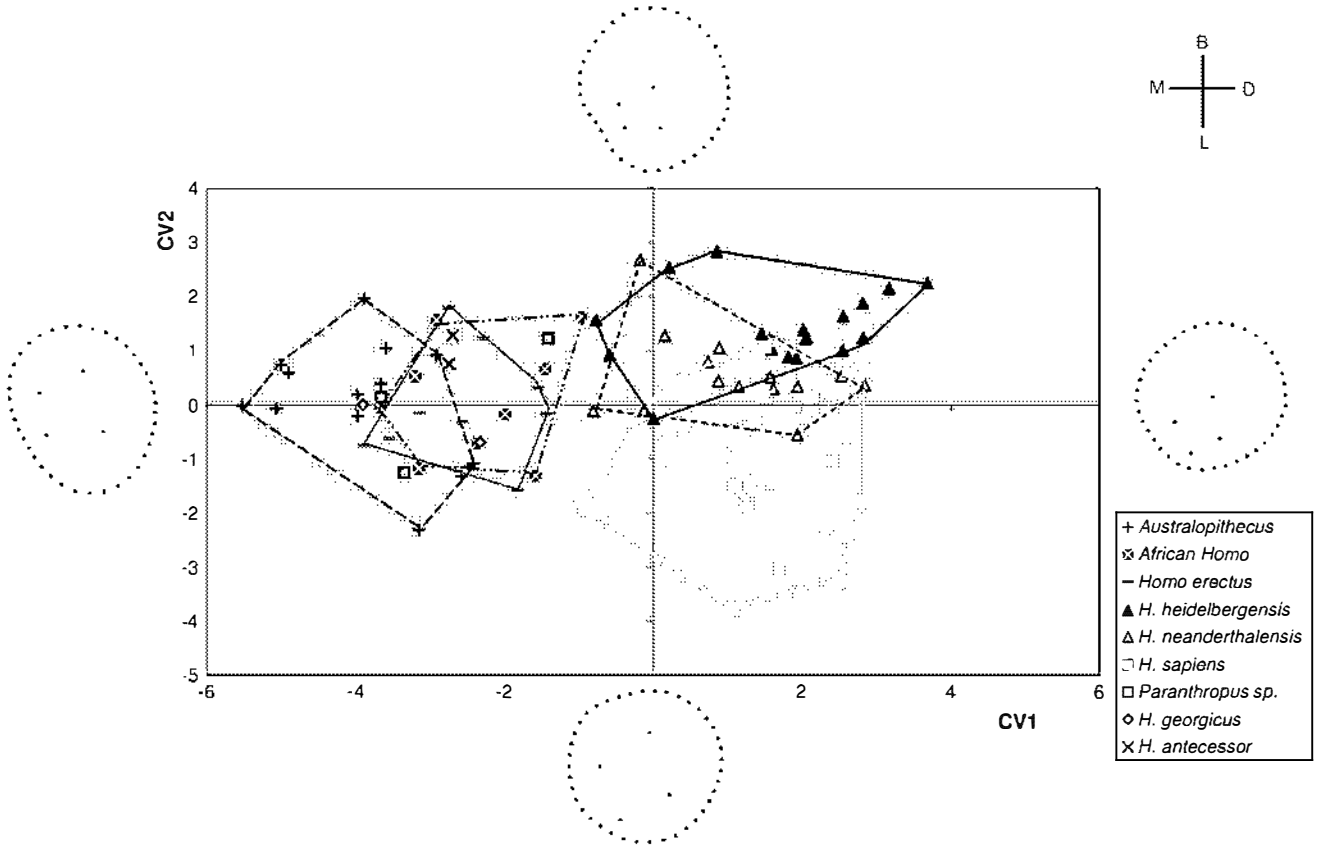

Fig. 4. Canonical variates analysis. Individual P_3 crowns are plotted in a way that maximizes the morphological differences among the a priori established groups (see text for explanation). As can be observed, apart from a better discrimination among species, no substantial differences are shown among the relative warps analysis and the canonical variates analysis. Specimens not included in the CVA were later assigned to one of the included groups to determine their affinity and they were plotted in the CVA graph (see text for explanation). The P_3 shape corresponding to each extreme of the CVs was obtained with TpsRegr software (Rohlf, 1998c).

and *H. erectus*) and the more recent taxa. All Asian and African specimens have negative values for CV1, whereas almost all of the European specimens and *H. sapiens* (with the exception of three *H. heidelbergensis* from Arago, three *H. neanderthalensis*, and one *H. sapiens* specimens) have positive values.

The premolars in the pooled *Australopithecus sp.* sample have the most extreme negative scores for CV1, and they display a slight trend to plot in positive values with respect to CV2. All African *Homo* and *H. erectus* specimens also plot in the negative half of CV1 and they share part of the morphospace with *Australopithecus*. Along CV2 there is substantial overlap between African *Homo* and *H. erectus*.

The *H. heidelbergensis* sample is almost entirely (15 of 18 individuals) located in the upper right quadrant of the CVA plot. This position corresponds to positive values for both CVs. However, Arago individuals display either negative scores for CV1 (Arago 71 and Arago 75) or negative scores for both CV1 and CV2 (Arago 13). The Atapuerca-Sima de los Huesos sample has the most positive values for CV2. *H. neanderthalensis* has mainly positive values for CV1 and CV2, although they are not as extreme as in Sima de los Huesos sample. Finally, *H. sapiens* is mainly located in the lower right quadrant of the CVA plot with two *H. neanderthalensis* specimens situated close to the zero value for CV2. Thus, *H. sapiens* specimens can be discriminated from *H. heidelbergensis* and *H. neanderthalensis* along CV2, whereas the earliest groups (*Australopithecus sp.*, African *Homo*, and *H. erectus*) can be discriminated from the later *Homo* species (*H. heidelbergensis, H. neanderthalensis*, and *H. sapiens*) along CV1.

A moderately high percentage of *Australopithecus* sp., *H. heidelbergensis*, and *H. sapiens* specimens are correctly assigned to their group, whereas the other groups have assignment percentages that are below 70% (Table 4). Nevertheless, it is important to note that no individual of the first three groups (*Australopithecus sp.*, African *Homo*, and *H. erectus*) is wrongly assigned to any of the European fossil groups or to *H. sapiens*. Similarly, just two *H. heidelbergensis* specimens (both from Arago) and one *H. neanderthalensis* (but not any *H. sapiens*) are wrongly assigned to one of the early African or Asian groups.

Table 3
Canonical variates analysis (CVA)

Function	Eigenvalue	% explained variance	% cumulative variance
1	4.906	80.7	80.7
2	0.785	12.9	93.6
3	0.318	5.2	98.9
4	0.068	1.1	100
5	0.000	0	100

Table 4
Assignment test results based on the canonical variates analysis

	% correct assignment	Number of correctly assigned specimens
Australopithecus sp.	76.9	10/13
African *Homo*	66.7	6/9
H. erectus	70.0	7/10
H. heidelbergensis	83.3	15/18
H. neanderthalensis	66.7	10/15
H. sapiens	70.6	24/34

The specimens not included in the CVA were later assigned to one of the other groups in order to ascertain their morphological affinities. Two *Paranthropus* specimens were assigned to *Australopithecus sp.* (KNM-ER 3230 and TM1517), whereas the other one (OMO-L427-7) was classified as African *Homo*. Premolars from Dmanisi were assigned either to *Australopithecus sp.* (D2735) or African *Homo* (D211). Eventually, both *H. antecessor* specimens were classified as *H. erectus*.

Allometry

The multivariate regression of the partial warps and uniform component scores against the centroid size revealed a significant allometric effect ($p < 0.0001$), so that 17.3% of the shape change can be linked to differences in overall size. Hominins with small premolar crowns tend to have a circular and symmetrical outline combined with a compressed and lingually-located occlusal polygon, whereas larger premolars present strongly asymmetrical outlines as a consequence of a conspicuous and well-developed talonid (Fig. 5). The occlusal polygons of the latter tend to occupy a larger proportion of the occlusal surface, and the tips of the protoconid and metaconid are mesially displaced.

Early African and Asian species present significantly ($p < 0.0001$) higher centroid sizes, with values that are always above 2.9 (*A. afarensis*: 2.93; *A. africanus*: 3.35; *Paranthropus*: 3.62; *H. habilis*: 3.01; *H. ergaster*: 2.90; *H. erectus*: 3.02), whereas the more recent hominin taxa have values below 2.7 (*H. heidelbergensis*: 2.54; *H. neanderthalensis*: 2.64; *H. sapiens*: 2.26). Thus, the differences in first premolar morphology that separate earlier from more recent hominins could be partially related to an allometric change from the largest premolars to the smallest ones. With regard to the allometric effect, the differences between the P_3 morphology of earlier and later hominins can be summarized by the relative migration of the protoconid apex toward the center of the tooth (allometric decrease of the protoconid-metaconid axis), lingual displacement of the distal fovea (relative shortening of the distal fovea-mesial fovea axis), an allometric reduction of the talonid, and a relative extension of the distobucal outline that gives the later hominin premolars an approximately round contour (Fig. 5).

Discussion

Specific differences

This analysis of P_3 crown morphology using geometric morphometrics has demonstrated clear differences between the early African and Asian hominin taxa, and later *Homo* species (*H. heidelbergensis*, *H. neanderthalensis*, and *H. sapiens*). The morphospaces of the premolars of the early African and Asian hominins overlap, but are separate from *H. heidelbergensis*, *H. neanderthalensis*, and *H. sapiens*. We infer that the more primitive morphology for the genus *Homo* consists of a strongly asymmetrical occlusal outline, a conspicuous talonid, and an occlusal polygon that is always larger than that seen in *H. heidelbergensis* and *H. neanderthalensis*. From this shape, two derived morphologies originate (Fig. 6). One corresponds to *H. sapiens* and consists of a symmetrical and circular premolar outline with a weak or absent talonid. The occlusal polygon is large and centrally located due to the buccally-displaced protoconid tip. The second derived morphology is seen in *H. heidelbergensis* and *H. neanderthalensis*. The first premolar of these taxa have a small occlusal polygon with the apex of the protoconid located towards the center of the tooth. As a consequence, Neandertal and *H. heidelbergensis* premolars have a small and lingually-displaced occlusal polygon located within a symmetrical, or slightly asymmetrical, occlusal outline. When present, the talonid is small and forms a smooth protrusion on the distolingual aspect of the crown. Additionally, the results of the CVA show that both Sima de los Huesos and *H. neanderthalensis* samples often present dissimilarity in the mesial and distal sides of the lingual outline, with the distal side being convex and the mesial side being concave. Although this morphology is also seen in *H. sapiens*, it is much more frequent in the European Pleistocene populations.

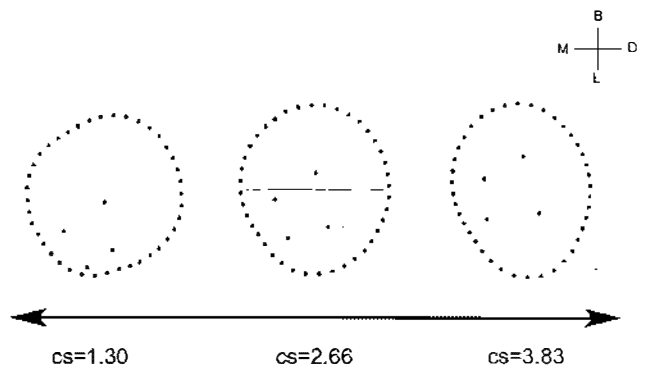

Fig. 5. Morphological variants corresponding to the lowest, mean, and highest centroid size. As it can be noted, the allometric factor related to the early-modern shape change is characterized by relative decrease of the talonid and the lengths among cusps and foveae, as well as by a relative buccodistal expansion.

Differences in P_3 morphology among African Pliocene and lower Pleistocene species were proposed by Wood and Uytterschaut (1987). They emphasized *Paranthropus* (mainly *P. boisei*) having relatively large talonids when compared to *A. africanus*, *H. habilis*, and *H. ergaster* that gave rise to a more asymmetrical outline. Suwa et al. (1996) remarked on an African hominin trend (*A. afarensis-A. africanus*-early *Homo*) of losing the primitive features associated with sectorial first premolars. However, these differences are relatively small when compared to the differences between earlier and later fossil hominins. The inclusion of *H. heidelbergensis*, *H. neanderthalensis*, and *H. sapiens* has relatively reduced the distinction within the more archaic groups. The morphological extremes identified by Wood and Uytterschaut (1987) by means of Procrustes superimposition, and exemplified by the contrast between KNM-ER 992 and KNM-ER 3230, are also picked up in our own PCA analysis (Fig. 3), where these two specimens have relatively distant positions within the variability of the archaic groups. The *A. afarensis* specimens included in this analysis and not included by Wood and Uytterschaut (1987) show substantial variation in the degree of molarization of their P_3s, with premolars that range from a nearly sectorial conformation (A.L. 128-23) to clearly bicuspid ones (A.L. 333w-60) (Leonard and Hegmon, 1987), but all of them tend to display an asymmetrical outline with an occlusal polygon not as large as seen in other early hominins. Still, differences among African specimens are difficult to ascertain given the small sample sizes of these groups in our study.

Paranthropus premolars have been defined as derived with respect to early hominin species (e.g., Wood and Uytterschaut, 1987; Suwa, 1988; Suwa et al., 1996; Bailey and Wood, 2007), and this morphocline is also suggested by our own results, although it is not so evident when early African hominins are compared with middle and late Pleistocene species. However, a formal cladistic analysis has not been carried out, and the size of the *Paranthropus* sample is still too small to make formal conclusions with respect to this group. Despite being derived with respect to *Australopithecus* and African *Homo*, *Paranthropus* first premolars are assigned to these groups because they better accommodate the variability of the *Paranthropus* specimens, located at the extreme of the variation of the groups included in the CVA.

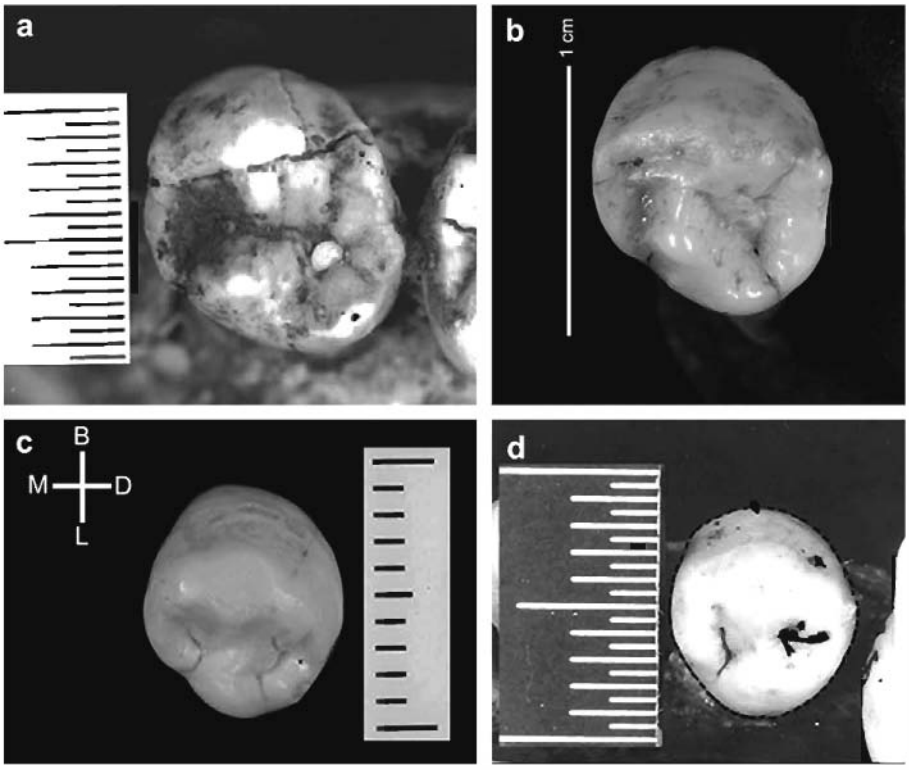

Fig. 6. Morphological comparison of the described shapes: (a) ER 1802 and (b) ATD6-3 show the typical morphology of earlier hominins, whereas (c) AT-1466 and (d) Coimbra226 illustrate the derived morphology. Size ratios are approximately kept among the four pictures.

In neither of the PCA nor CVA graphs is there a hominin taxon with a morphology that is clearly intermediate between the earlier and later groups. Some *H. ergaster* specimens and one *H. georgicus* individual are close to the distribution areas of *H. heidelbergensis, H. neanderthalensis*, and *H. sapiens*, but the morphological variability within the former groups is high. These specimens show a slight reduction of the talonid and a less asymmetrical outline compared to earlier African specimens. However, when we use the CVA to assign the Dmanisi specimens to one of the most represented groups, one of them (D211) is classified as African *Homo* and the other (D2735) as *Australopithecus sp.*, highlighting their similarity with early *Homo* and even with *Australopithecus* in some traits by retaining plesiomorphic characters (Rightmire et al., 2006; Lordkipanidze et al., 2007; Martinón-Torres et al., in press).

The absence of overlap between the distribution areas of *H. ergaster* and *H. erectus* in the PCA, with *H. ergaster* plotting closer to the morphospace of the later *Homo* taxa, would support the different specific allocation of African and Asian lower Pleistocene specimens (e.g., Wood, 1984,1994; Wood and Richmond, 2000). In the case of *H. erectus*, there are slight differences between the Chinese (from Zhoukoudian) and Javanese (from Sangiran and Trinil) specimens. Zhoukoudian premolars tend to show lower values for both PC2 and CV2 than do Javan individuals, highlighting the Sangiran trend to display a slightly more asymmetrical P_3 within the *H. erectus* group. Zhoukoudian 20 and 80 belong to a mixed collection of small fossil orang-utan and hominin teeth (Schwartz and Tattersall, 2003). Although we have kept the assignment to *H. erectus* proposed by Weidenreich (1937), both the general morphology and the location of these premolars in the PCA plot (at the extreme of variation of the studied hominin sample) could better support their classification as non-hominin. However, a comparison with an ape sample would be required to confirm that.

The *H. antecessor* specimens are characterized by derived P_4 and M^1 shapes (Martinón-Torres et al., 2006; Gómez-Robles et al., 2007), but they retain primitive P_3 shapes, with morphologies similar to those found in early African and Asian species. The use of the CVA to include these specimens in one of the most-represented groups of the sample associates them with Asian *H. erectus.* This association could support the phylogenetic relationship between Asian and European Pleistocene populations as proposed by some authors (Dennell and Roebroeks, 2005, Martinón-Torres et al., 2007), but the restricted ability of P_3 to taxonomically allocate isolated specimens prevents us from drawing final conclusions.

The Arago specimens (Arago 13, 71, and 75) plot outside the distribution area of the Atapuerca-Sima de los Huesos premolars. Interestingly, Arago premolars have slightly different morphologies, and, despite sharing the same small area of the morphospace, they show affinities with different groups (Bermúdez de Castro et al., 2003): Arago 71 is situated with the early hominin taxa (due to its asymmetrical shape and large occlusal polygon [left upper quadrant of Fig. 3]); Arago 13, located at the confluence of the four quadrants (point 0) of Fig. 3, is more similar to later hominins (because of its symmetrical shape with a centered and large occlusal polygon); and Arago 75 plots in an intermediate position between modern and earlier groups, showing a medium-sized talonid and a central occlusal polygon.

Although the *H. neanderthalensis* and *H. heidelbergensis* distributions overlap, the Sima de los Huesos first premolars plot at the extreme of PC1. In general, *H. heidelbergensis* from Sima de los Huesos and *H. neanderthalensis* have been described as having similar dental traits, the only difference being that *H. neanderthalensis* presents higher degrees of expression for some of those traits (e.g., Bermúdez de Castro, 1987, 1988, 1993; Martinón-Torres, 2006; Martinón-Torres et al., 2006; Gómez-Robles et al., 2007). It is interesting to note that, in this particular tooth, Sima de los Huesos specimens display a morphology that is even more pronounced than the classic Neandertals. This may reflect a morphological particularity of this biological population as its marked reduction of the size of their posterior teeth (Bermúdez de Castro and Nicolás, 1995). The similarities in P_3 shape, along with other

dental traits (Bermúdez de Castro, 1987, 1988, 1993; Martinón-Torres, 2006; Martinón-Torres et al., 2006; Gómez-Robles et al., 2007), support the hypothesis that there is a close phylogenetic relationship between the hominins of Atapuerca-Sima de los Huesos and the late Pleistocene classic Neandertals (e.g., Arsuaga et al., 1993, 1997; Bermúdez de Castro, 1993; Martinón-Torres, 2006).

As stated earlier, there are no significant differences between the distribution areas of the two modern human samples analyzed in this study. However, three out of the four early modern humans studied (Qafzeh 9 and 11, and Grotte des Enfants 6) plot at the extreme of the variability of the modern human sample (lowest values for PC1 and PC2).

Allometry

An allometric effect accounts for 17.3% of the shape differences among the hominins. Given that the P_3s of earlier hominin species are generally larger than that of the more recent groups (Bermudez de Castro and Nicolas, 1995, 1996), the archaic to modern morphological gradient could be partially linked to a size change from large to small. However, that size change is not isometric. The reduction of the overall size of the P_3 crown is accompanied by a more significant reduction of the distance between the protoconid and metaconid apices and, specially, of the talonid area (Fig. 5). In addition, the relative extension of the distobuccal outline gives small P_3s a more rounded contour.

Previous papers on P_3 morphology have not found clear evidence of allometry in the morphology of this tooth. Wood and Uytterschaut (1987) did not find any significant correlation between talonid size and overall crown size in any of the groups they studied (*A. africanus, P. robustus, P. boisei*, and *H. habilis*). Leonard and Hegmon (1987) proposed that in *A. afarensis* there is an association between molarization of the P_3 and premolar size, but only for the female specimens. Similarly, Suwa et al. (1996) assumed that the relative cusp proportions of *Paranthropus* were not exclusively the result of an allometric change from non-robust species. Our analysis of a more comprehensive sample that includes comparatively smaller premolars, such as those from *H. heidelbergensis, H. neanderthalensis*, and *H. sapiens*, suggests that there is an allometric component affecting in some degree the evolution of P_3 morphology within the hominin clade.

Evolutionary implications

Wood and Uytterschaut (1987) showed that *Paranthropus* premolars, with the most asymmetrical shape, tend to have additional cusps on the talonid. This contrasts with *Australopithecus* and early *Homo* specimens, which have a lower frequency of extra cusps, and which have relatively less asymmetrical P_3 crown outlines. These differences in the degree of asymmetry are masked when more recent (and symmetrical) specimens are included in the analysis. Although initially we could correlate the presence of additional cusps with a well-developed talonid, *H. sapiens* tend to keep their symmetrical and rounded outline even when extralingual cusps are developed (Kraus and Furr, 1953; Scott and Turner, 1997; Bailey, 2002b; Martinón-Torres, 2006). Therefore, even though the presence and the number of additional cusps is highly variable and useful for lower taxonomic distinctions (Jernvall and Jung, 2000), the disposition of the main cusps and the general morphology of the outline should be more powerful tools for taxonomic discrimination.

It has been demonstrated that the morphogenesis of the upper and lower dentition are under the control of different genetic programs (Thomas et al., 1997; Ferguson et al., 1998; McCollum and Sharpe, 2001). This could explain why M^1 tends to retain a primitive morphology in *H. sapiens* (Gómez-Robles et al., 2007), whereas P_3 crowns are derived in this species. Although it has been proposed that the teeth of the same class have a correlated expression (Nichol, 1990; Irish, 2005), the evolutionary trend also differs between the two types of lower premolar, since *H. neanderthalensis* apparently retains a primitive P_4 morphology (Martinón-Torres et al., 2006), whereas the shape of their P_3 is clearly derived (this study). Thus, if the different trends in the P_3 and P_4 were to be confirmed, it could be hypothesized that they are influenced by different morphogenetic fields (Mizoguchi, 1981; Kieser and Groeneveld, 1987; Bermúdez de Castro and Nicolás, 1996). However, the classical concept of morphogenetic fields of dentition (Butler, 1939; Dahlberg, 1945) seemingly represents the concerted action of a series of individual molecular fields (Line, 2001), affecting different teeth.

The results of the assignment test do not reveal a strong discriminative power of the P_3 morphology in determining the taxonomical affinities of the individuals. Notwithstanding, the clear differences among early hominin species and later *Homo* groups may suggest the existence of ecological and evolutionary factors underlying these shape changes. Genetic drift could be a plausible mechanism for explaining the described shape differences (Lynch, 1989; Relethford, 1994; Roseman, 2004; Roseman and Weaver, 2004; Weaver et al., 2007), although the morphological distinction in P_3 morphology between earlier and later hominin species compels us to consider the existence of evolutionary advantages of the described shapes in each case that probably would not have adaptive benefits per se, but which could be correlated with other skeletal changes (McCollum and Sharpe, 2001).

Conclusions

This geometric morphometric study of the hominin P_3 crown morphology has revealed a noticeable change in shape from the earliest hominin species sampled to the later *Homo* species. The inferred primitive morphology, typical of *Australopithecus* and early *Homo* individuals, as well as of Asian *H. erectus* specimens, consists of a strongly asymmetrical outline combined with a large and well-developed talonid and a generally expanded occlusal polygon. The two derived morphologies both have an approximately symmetrical outline with a reduced or absent talonid. In *H. neanderthalensis* and *H. heidelbergensis* the P_3 crowns have a small and lingually-located occlusal polygon, whereas in *H. sapiens* specimens the occlusal polygon is larger and more central, and the outline is approximately circular.

The evidence of a significant inter-specific allometric effect on the shape change and the obvious separation between the earliest hominin species of the sample and the later ones (*H. heidelbergensis, H. neanderthalensis*, and *H. sapiens*) suggest that there may be an ecological influence on P_3 morphology.

When the results of this study of the first premolar morphology is compared to the results of studies of other teeth, it is evident that a simple explanation cannot be applied to these accumulated findings, but that it is necessary to consider a complex mosaic pattern for the evolution of the human dentition.

Acknowledgements

We are grateful to all members of the Atapuerca research team, especially to the Sima de los Huesos excavation team for their arduous and exceptional contribution. We also thank I. Tattersall, G. Sawyer, and G. García from the American Museum of Natural History, New York; O. Kullner, B. Denkel, F. Schrenk and Luca Fiorenza from Senckenberg Institute, Frankfurt, Germany; J. de Vos from Naturalis Museum, Leiden, the Netherlands; D. Lordkipanidze, A. Vekua, G. Kiladze, and A. Margvelashvili from the Georgian

National Museum; J. Svoboda and M. Oliva from the Institute of Archaeology-Paleolithic and Paleoethnology Research Center, Dolní Vestonice, Czech Republic; G. Manzi from Università La Sapienza, Rome; E. Cunha from Universidade de Coimbra and M.A. de Lumley from Centre Europeen de Recherches, Tautavel, France for providing access to the studied material and their helpful assistance when examining it. Special thanks to James Rohlf at SUNY, Stony Brook, for his advice regarding methodological aspects. We specially grateful to Ana Muela for her technical support and for photographing part of the sample. We are indebted to Susan Antón for her thorough editing of the manuscript and her helpful comments, as well as those provided by three anonymous referees, which greatly improved the manuscript. We are specially grateful to Gisselle García from the AMNH who has kindly provided the information on the AMNH modern collection. Thanks to Miguel Botella from the Laboratory of Anthropology of the Universidad de Granada for his continuous support. Special thanks to David Sánchez for his invaluable help with technical questions. This research was supported by funding from the Dirección General de Investigación of the Spanish M.E.C., Project No. CGL2006-13532-C03-03/BTE, Spanish Ministry of Science and Education, Fundación Atapuerca, and Fundación Duques de Soria. Fieldwork at Atapuerca is supported by Consejería de Cultura y Turismo of the Junta de Castilla y León. A. G-R. has the benefit of a predoctoral FPU grant of the Spanish MEC. This research was partly carried out under the Cooperation Treaty between Spain and the Republic of Georgia, hosted by the Fundación Duques de Soria and the Georgian National Museum.

References

Adams, D.C., Rohlf, F.J., Slice, D.E., 2004. Geometric morphometrics: ten years of progress following the 'Revolution'. Ital. J. Zool. 71, 5–16.

Albrecht, G.H., 1980. Multivariate analysis and the study of form with special reference to canonical variate analysis. Am. Zool. 20, 679–693.

Arsuaga, J.L., Martínez, I., Gracia, A., Carretero, J.M., Carbonell, E., 1993. Three new human skulls from the Sima de los Huesos Middle Pleistocene site in Sierra de Atapuerca, Spain. Nature 362, 534–537.

Arsuaga, J.L., Martínez, I., Gracia, A., Lorenzo, C., 1997. The Sima de los Huesos crania (Sierra de Atapuerca, Spain): a comparative study. J. Hum. Evol. 33, 219–281.

Bailey, S.E., 2000. Dental morphological affinities among late Pleistocene and recent humans. Dent. Anthropol. 14, 1–8.

Bailey, S.E., 2002a. A closer look at Neandertal postcanine dental morphology: I. the mandibular dentition. New Anat. 269, 148–156.

Bailey, S.E., 2002b. Neandertal dental morphology: implications for modern human origins. Ph.D. Dissertation, Arizona State University.

Bailey, S.E., 2004. A morphometric analysis of maxillary molar crowns of Middle-Late Pleistocene hominins. J. Hum. Evol. 47, 183–198.

Bailey, S.E., Lynch, J.M., 2005. Diagnostic differences in mandibular P4 shape between Neandertals and anatomically modern humans. Am. J. Phys. Anthropol. 126, 268–277.

Bailey, S.E., Pilbrow, V.C., Wood, B.A., 2004. Interobserver error involved in independent attempts to measure cusp base areas of Pan M1s. J. Anat. 205, 323–331.

Bailey, S.E., Wood, B.A., 2007. Trends in postcanine occlusal morphology within the hominin clade: the case of Paranthropus. In: Bailey, S.E., Hublin, J.-J. (Eds.), Dental Perspectives on Human Evolution. Springer-Verlag, Berlin, pp. 53–64.

Bastir, M., 2004. Análisis de morfometría geométrica de la variación e integración morfológica en el cráneo humano y sus implicaciones para los homínidos de Atapuerca-SH y la evolución de los Neandertales. Ph.D. Dissertation, Universidad Autónoma de Madrid.

Bastir, M., Rosas, A., O'Higgins, P., 2006. Craniofacial levels and the morphological maturation of the human skull. J. Anat. 209, 637–645.

Bermúdez de Castro, J.M., 1987. Morfología comparada de los dientes humanos fósiles de Ibeas (Sierra de Atapuerca, Burgos). Estudios Geológicos 43, 309–333.

Bermúdez de Castro, J.M., 1988. Dental remains from Atapuerca/Ibeas (Spain) II. Morphology. J. Hum. Evol. 17, 279–304.

Bermúdez de Castro, J.M., 1993. The Atapuerca dental remains: new evidence (1987–1991 excavations) and interpretations. J. Hum. Evol. 24, 339–371.

Bermúdez de Castro, J.M., Arsuaga, J.L., Carbonell, E., Rosas, A., Martínez, I., Mosquera, M., 1997. A hominid from the Lower Pleistocene of Atapuerca, Spain: possible ancestor to Neandertals and modern humans. Science 276, 1392–1395.

Bermúdez de Castro, J.M., Martinón-Torres, M., Sarmiento, S., Lozeno, M., 2003. Gran Dolina-TD6 versus Sima de los Huesos dental samples from Atapuerca: evidence of discontinuity in the European Pleistocene population? J. Archaeol. Sci. 30, 1421–1428.

Bermúdez de Castro, J.M., Nicolás, M.E., 1995. Posterior dental size reduction in hominids: the Atapuerca evidence. Am. J. Phys. Anthropol. 96, 335–356.

Bermúdez de Castro, J.M., Nicolás, E., 1996. Changes in the lower premolar-size sequence during hominid evolution: phylogenetic implications. Hum. Evol. 11, 205–215.

Bermúdez de Castro, J.M., Rosas, A., Nicolás, M.E., 1999. Dental remains from Atapuerca-TD6 (Gran Dolina site, Burgos, Spain). J. Hum. Evol. 37, 523–566.

Bernal, V., 2007. Size and shape analysis of human molars: comparing traditional and geometric morphometric techniques. Homo 58, 279–296.

Biggerstaff, R.H., 1969. The basal area of posterior tooth crown components: the assessment of within tooth variation of premolars and molars. Am. J. Phys. Anthropol. 31, 163–170.

Bookstein, F.L., 1989. Principal warps: thin-plate splines and the decomposition of deformations. IEEE Trans. Pattern. Anal. Mach. Intell. 11, 567–585.

Bookstein, F.L., 1991. Morphometric Tools for Landmark Data. Cambridge University Press, Cambridge.

Bookstein, F.L., 1996a. Combining the tools of geometric morphometrics. In: Marcus, L.F., Corti, M., Loy, A., Naylor, G.J.P., Slice, D. (Eds.), Advances in Morphometrics. Plenum Press, New York, pp. 131–151.

Bookstein, F.L., 1996b. Applying landmark methods to biological outline data. In: Mardia, K.V., Gill, C.A., Dryden, I.L. (Eds.), Image Fusion and Shape Variability Techniques. Leeds University Press, Leeds.

Bookstein, F.L., 1997. Landmark methods for forms without landmarks: morphometrics of group differences in outline shape. Med. Image Anal. 1, 225–243.

Bookstein, F.L., Sampson, P.D., Connor, P.D., Streissguth, A.P., 2002. Midline corpus callosum is a neuroanatomical focus of fetal alcohol damage. Anat. Rec. New Anat. 269, 162–174.

Bookstein, F.L., Schäfer, K., Prossinger, H., Seidler, H., Fieder, M., Stringer, C., Weber, G.W., Arsuaga, J.L., Slice, D.E., Rohlf, F.J., Recheis, W., Mariam, A.J., Marcus, L.F., 1999. Comparing frontal cranial profiles in archaic and modern *Homo* by morphometric analysis. Anat. Rec. New Anat. 257, 217–224.

Butler, P.M., 1939. Studies of the mammalian dentition: differentiation of the post-canine cheek dentition. Proc. Zool. Soc. Lond. 109B, 1–36.

Coppens, Y., 1977. Evolution morpholgique de la première prémolaire inférieure chez certains Primates supérieurs. C.R. Acad. Sci. Paris, Ser D 285, 1299–1302.

von Cramon-Taubadel, N., Frazier, B.C., Lahr, M.M., 2007. The problem of assessing landmark error in geometric morphometrics: theory, methods, and modifications. Am. J. Phys. Anthropol. 134, 24–35.

Dahlberg, A.A., 1945. The changing dentition in man. J. Am. Dent. Assoc. 32, 676–690.

Dennell, R., Roebroeks, W., 2005. An Asian perspective on early human dispersal from Africa. Nature 438, 1099–1104.

Dryden, I.L., Mardia, K.V., 1998. Statistical Shape Analysis. Wiley, Chichester.

Dubois, E., 1894. *Pithecanthropus erectus*: eine Menschenaehnlich Uebergangsform aus Java. Landsdrukerei, Batavia.

Ferguson, C.A., Tucker, A.S., Christensen, L., Lau, A.L., Matzuk, M.M., Sharpe, P.T., 1998. Activin is an essential early mesenchymal signal in tooth development that is required for patterning of the murine dentition. Genes Dev. 12, 2636–2649.

Foley, R., Lahr, M., 1997. Mode 3 technologies and the evolution of modern humans. Camb. Archaeol. J. 7, 3–36.

Frieß, M., 2003. An application of the relative warps analysis to problems in human paleontology: with notes on raw data quality. Image Anal. Stereol. 22, 63–72.

Gabunia, L.K., Lumley, M.A., deVekua, A., Lordkipanidze, D., de Lumley, H., 2002. Découverte dun nouvel hominidé a Dmanisi (Transcaucasie, Géorgie). C.R. Palevol. 1, 243–253.

Gharaibeh, W., 2005. Correcting for the effect of orientation in geometric morphometric studies of side-view images of human heads. In: Slice, D.E. (Ed.), Modern Morphometrics in Physical Anthropology. Kluwer Academic/Plenum Publishers, New York, pp. 117–143.

Gómez-Robles, A., Martinón-Torres, M., Bermúdez de Castro, J.M., Margvelashvili, A., Bastir, M., Arsuaga, A., Pérez-Pérez, A., Estebaranz, F., Martínez, L., 2007. A geometric morphometric analysis of hominin upper first molar shape. J. Hum. Evol. 53, 272–285.

Grine, F.E., Franzen, J.L., 1994. Fossil hominid teeth from the Sangiran Dome (Java, Indonesia). Cour. Forsch. Inst. Senckenberg 171, 75–103.

Groves, C.P., Mazák, V., 1975. An approach to the taxonomy of the Hominidae: gracile Villafranchian hominids of Africa. Casopis Min. Geol. 20, 225–247.

Gunz, P., Mitteroecker, P., Bookstein, F.L., 2005. Semilandmarks in three dimensions. In: Slice, D. (Ed.), Modern Morphometrics in Physical Anthropology. Kluwer Academic/Plenum Publishers, New York, pp. 73–98.

Hammer, O., Harper, D., 2006. Paleontological Data Analysis. Blackwell Publishing, Oxford.

Harris, E.F., Dinh, D.P., 2006. Intercusp relationships of the permanent maxillary first and second molars in American whites. Am. J. Phys. Anthropol. 130, 514–528.

Harvati, K., 2003. The Neanderthal taxonomic position: models of intra- and inter-specific craniofacial variation. J. Hum. Evol. 44, 107–132.

Hlusko, L.J., 2004. Protostylid variation in Australopithecus. J. Hum. Evol. 46, 579–594.

Hlusko, L.J., Do, N., Mahaney, M.C., 2007. Genetic correlations between mandibular molar cusp areas in baboons. Am. J. Phys. Anthropol. 132, 445–454.

Irish, J.D., 1993. Biological affinities of Late Pleistocene through modern African aboriginal populations: the dental evidence. Ph.D. Dissertation, Arizona State University.

Irish, J.D., 1997. Characteristic high- and low-frequency dental traits in sub-Saharan African populations. Am. J. Phys. Anthropol. 102, 455–467.
Irish, J.D., 1998. Ancestral dental traits in recent sub-Saharan Africans and the origins of modern humans. J. Hum. Evol. 34, 81–98.
Irish, J.D., 2005. Population continuity vs. discontinuity revisited: dental affinities among late Paleolithic through Christian era Nubians. Am. J. Phys. Anthropol. 128, 520–535.
Irish, J.D., Guatelli-Steinberg, D., 2003. Ancient teeth and modern human origins: an expanded comparison of African Plio-Pleistocene and recent world dental samples. J. Hum. Evol. 45, 113–144.
Jernvall, J., Jung, H.-S., 2000. Genotype, phenotype, and developmental biology of molar tooth characters. Yearb. Phys. Anthropol. 43, 171–190.
Kieser, J.A., Groeneveld, H.T., 1987. Tooth size and arcadal length correlates in man. Int. J. Anthropol. 2, 37–46.
Klingenberg, C.P., 1998. Heterochrony and allometry: the analysis of evolutionary change in ontogeny. Biol. Rev. 73, 79–123.
Kraus, B.S., Furr, M.L., 1953. Lower first premolars. Part I. A definition and classification of discrete morphologic traits. J.D. Res. 32, 554–564.
Lahr, M., Foley, R., 1998. Towards a theory of modern human origins: geography, demography, and diversity in recent human evolution. Yearb. Phys. Anthropol. 41, 137–176.
Leonard, W.R., Hegmon, M., 1987. Evolution of P3 morphology in *Australopithecus afarensis*. Am. J. Phys. Anthropol. 73, 41–63.
Line, S.R., 2001. Molecular morphogenetic fields in the development of human dentition. J. Theoret. Biol. 211, 67–75.
Lockwood, C.A., Kimbel, W.H., Johanson, D.C., 2000. Temporal trends and metric variation in the mandibles and dentition of *Australopithecus afarensis*. J. Hum. Evol. 39, 23–55.
Lordkipanidze, D., Jashashvili, T., Vekua, A., Ponce de León, M.S., Zollikofer, C.P.E., Rightmire, G.P., Pontzer, H., Ferring, R., Oms, O., Tappen, M., Bukhsianidze, M., Agusti, J., Kahlke, R., Kiladze, G., Martinez-Navarro, B., Mouskhelishvili, A., Inoradse, M., Rook, L., 2007. Postcranial evidence from early *Homo* from Dmanisi, Georgia. Nature 449, 305–310.
Lynch, M., 1989. Phylogenetic hypotheses under the assumption of neutral quantitative-genetic variation. Evolution 43, 1–17.
Manzi, G., 2004. Human evolution at the Matuyama-Brunhes boundary. Evol. Anthropol. 13, 11–24.
Martinón Torres, M., 2006. Evolución del aparato dental en homínidos: estudio de los dientes humanos del Pleistoceno de la Sierra de Atapuerca (Burgos). Ph.D. Dissertation, Universidad de Santiago de Compostela.
Martinón-Torres, M., Bastir, M., Bermúdez de Castro, J.M., Gómez, A., Sarmiento, S., Muela, A., Arsuaga, J.L., 2006. Hominin lower second premolar morphology: evolutionary inferences through geometric morphometric analysis. J. Hum. Evol. 50, 523–533.
Martinón-Torres, M., Bermúdez de Castro, J.M., Gómez-Robles, A., Arsuaga, J.L., Carbonell, E., Lordkipanidze, D., Manzi, G., Margvelashvili, A., 2007. Dental evidence on the hominin dispersals during the Pleistocene. Proc. Natl. Acad. Sci. U.S.A. 104, 13279–13282.
Martinón-Torres, M., Bermúdez de Castro, J.M., Margvelashvili, A., Gómez-Robles, A., Lordkipanidze, D., Vekua, A. Dental remains from Dmanisi (Republic of Georgia): anatomical description and comparative study. J. Hum. Evol. in press. doi:10.1016/j.jhevol.2007.12.008
McCollum, M.A., Sharpe, P.T., 2001. Developmental genetics and early hominid craniodental evolution. BioEssays 23, 481–493.
Mizoguchi, Y., 1981. Variation units in the human permanent dentition. Bull. Nat. Sci. Mus. Tokio 7, 29–39.
Moggi-Cecchi, J., Boccone, S., 2007. Maxillary molar cusp morphology of South African australopithecines. In: Bailey, S.E., Hublin, J.-J. (Eds.), Dental Perspectives on Human Evolution. Springer-Verlag, Berlin, pp. 53–64.
Moggi-Cecchi, J., Grine, F.E., Tobias, P.V., 2005. Early hominid dental remains from Members 4 and 5 of the Sterkfontein Formation (1966–1996 excavations): catalogue, individual associations, morphological descriptions and initial metrical analysis. J. Hum. Evol. 50, 239–328.
Mosimann, J.E., 1970. Size allometry: size and shape variables with characterizations of the lognormal and generalized gamma distributions. J. Am. Stat. Assoc. 65, 930–945.
Nichol, C.R., 1990. Dental genetics and biological relationships of the Pima Indians of Arizona. Ph.D. Dissertation, Arizona State University, Tempe.
Nolte, A.W., Sheets, H.D., 2005. Shape based assignment tests suggest transgressive phenotypes in natural sculpin hybrids (Teleostei, Scorpaeniformes, Cottidae). Frontiers in Zoology 2, 11.
Perez, S.I., Bernal, V., Gonzalez, P.N., 2006. Differences between sliding semi-landmark methods in geometric morphometrics, with an application to human craniofacial and dental variation. J. Anat. 208, 769–784.
Pilbrow, V., 2006. Population systematics of chimpanzees using molar morphometrics. J. Hum. Evol. 51, 646–662.
Relethford, J.H., 1994. Craniometric variation among modern human populations. Am. J. Phys. Anthropol. 95, 53–62.
Rightmire, G.P., 1998. Human evolution in the Middle Pleistocene: the role of *Homo heidelbergensis*. Evol. Anthropol. 6, 218–227.
Rightmire, G.P., Lordkipanidze, D., Vekua, A., 2006. Anatomical descriptions, comparative studies and evolutionary significance of the hominin skulls from Dmanisi, Republic of Georgia. J. Hum. Evol. 50, 115–141.
Rohlf, F.J., 1996. Morphometric spaces, shape components and the effects of linear transformations. In: Marcus, L.F. (Ed.), Advances in Morphometrics. Plenum Press, New York, pp. 117–128.
Rohlf, F.J., 1998a. TpsRelw. Ecology and Evolution, SUNY. Stony Brook, New York. http://life.bio.sunysb.edu/morph/.
Rohlf, F., 1998b. TpsRegr. Ecology and Evolution, SUNY. Stony Brook, New York. http://life.bio.sunysb.edu/morph/.
Rohlf, F., 1998c. TpsDig. Ecology and Evolution, SUNY. Stony Brook, New York. http://life.bio.sunysb.edu/morph/.
Rohlf, F.J., Slice, D., 1990. Extensions of the Procrustes method for the optimal superimposition of landmarks. Syst. Zool. 39, 40–59.
Roseman, C.C., 2004. Detection of interregionally diversifying natural selection on modern human cranial form by using matched molecular and morphometric data. Proc. Natl. Acad. Sci. U.S.A. 101, 12824–12829.
Roseman, C.C., Weaver, T.D., 2004. Multivariate apportionment of global human craniometric diversity. Am. J. Phys. Anthropol. 125, 257–263.
Sampson, P.D., Bookstein, F.L., Sheehan, H., Bolson, E.L., 1996. Eigenshape analysis of left ventricular outlines from contrast ventriculograms. In: Marcus, L.F., Corti, M., Loy, A., Naylor, G.J.P., Slice, D.E. (Eds.), Advances in Morphometrics. Plenum, New York, pp. 131–152.
Schoetensack, O., 1908. Der Unterkiefer des *Homo heidelbergensis* aus den Sanden von Mauer bei Heidelberg. Wilhelm Engelmann, Leipzig.
Schwartz, J.S., Tattersall, I., 2003. The human fossil record, vol. 2. Wiley-Liss, New York.
Scott, G.R., Turner II, C.G., 1997. The Anthropology of Modern Human Teeth: Dental Morphology and its Variation in Recent Human Populations. Cambridge University Press, Cambridge.
Sheets, H.D., 2001. Imp, integrated morphometric package. http://www.canisius.edu/~sheets/morphsoft.html.
Sheets, H.D., Keonbo, K., Mitchell, C.E., 2004. A combined landmark and outline-based approach to ontogenetic shape change in the Ordovician Trilobite *Triarthrus becki*. In: Elewa, A. (Ed.), Applications of Morphometrics in Paleontology and Biology. Springer, New York, pp. 67–81.
Singleton, M., 2002. Patterns of cranial shape variation in the Papionini (Primates: Cercopithecinae). J. Hum. Evol. 42, 547–578.
Stringer, C., 2002. Modern human origins: progress and prospects. Phil. Trans. R. Soc. Lond. B 357, 563–579.
Stringer, C., Hublin, J.J., 1999. New age estimates for the Swanscombe hominid, and their significance for human evolution. J. Hum. Evol. 37, 873–877.
Suwa, G., 1988. Evolution of the "robust" australopithecines in the Omo succession: evidence from mandibular premolar morphology. In: Grine, F.E. (Ed.), Evolutionary History of the "Robust" Australopithecines. Aldine de Gruyter, New York, pp. 199–222.
Suwa, G., White, T.D., Howell, F.C., 1996. Mandibular postcanine dentition from the Shungura Formation, Ethiopia: crown morphology, taxonomic allocations, and Plio-Pleistocene hominid evolution. Am. J. Phys. Anthropol. 101, 247–282.
Thomas, B.L., Tucker, A.S., Qui, M., Ferguson, C.A., Hardcastle, Z., Rubenstein, J.L., Sharpe, P.T., 1997. Role of Dlx-1 and Dlx-2 genes in patterning of the murine dentition. Development 124, 4811–4818.
Tobias, P.V., 1991. Olduvai Gorge. The Skulls, Endocasts and Teeth of *Homo habilis*. vol. 4: Parts V-IX. Cambridge University Press, Cambridge.
Turner II, C.G., 1969. Microevolutionary interpretations from the dentition. Am. J. Phys. Anthropol. 30, 421–426.
Turner II, C.G., Nichol, C.R., Scott, G.R., 1991. Scoring procedures for key morphological traits of the permanent dentition: the Arizona State University Dental Anthropology System. In: Kelley, M., Larsen, C. (Eds.), Advances in Dental Anthropology. Wiley Liss, New York, pp. 13–31.
Walker, A., Leakey, R.E., 1993. The Nariokotome *Homo erectus* Skeleton. Springer-Verlag, Harvard University Press, Harvard.
Weaver, T.D., Roseman, C.C., Stringer, C.B., 2007. Were Neandertal and modern human cranial differences produced by natural selection or genetic drift? J. Hum. Evol. 53, 135–145.
Weidenreich, F., 1937. The dentition of *Sinanthropus pekinensis*: a comparative odontography of the hominids. Palaeont. Sin. New Ser. D 1, 1–180.
White, T.D., Suwa, G., Simpson, S., Asfaw, B., 2000. Jaws and teeth of *Australopithecus afarensis* from Maka, Middle Awash, Ethiopia. Am. J. Phys. Anthropol 111, 45–68.
Wood, B.A., 1984. The origin of *Homo erectus*. Cour. Forsch. Inst. Senck. 69, 99–111.
Wood, B., 1992. Origin and evolution of the genus *Homo*. Nature 355, 783–790.
Wood, B.A., 1994. Taxonomy and evolutionary relationships of *Homo erectus*. Cour. Forsch. Inst. Senck. 171, 159–165.
Wood, B., Abbott, S.A., 1983. Analysis of the dental morphology of Plio-Pleistocene hominids I. Mandibular molars: crown area measurements and morphological traits. J. Anat. 136, 197–219.
Wood, B.A., Abbott, S.A., Graham, S.H., 1983. Analysis of the dental morphology of Plio-Pleistocene hominids II. Mandibular molars-study of cusp areas, fissure pattern and cross sectional shape of the crown. J. Anat. 137, 287–314.
Wood, B.A., Abbott, S.A., Uytterschaut, H., 1988. Analysis of the dental morphology of Plio-Pleistocene hominids IV. Mandibular postcanine root morphology. J. Anat. 156, 107–139.
Wood, B.A., Collard, M., 1999. The human genus. Science 284, 65–71.
Wood, B.A., Engleman, C.A., 1988. Analysis of the dental morphology of Plio-Pleistocene hominids V. Maxillary postcanine tooth morphology. J. Anat. 161, 1–35.
Wood, B.A., Richmond, B.G., 2000. Human evolution: taxonomy and paleobiology. J. Anat. 196, 19–60.
Wood, B.A., Uytterschaut, H., 1987. Analysis of the dental morphology of Plio-Pleistocene hominids III. Mandibular premolar crowns. J. Anat. 154, 121–156.
Zelditch, M.L., Swiderski, D.L., Sheets, H.D., Fink, W.L., 2004. Geometric Morphometrics for Biologists: A Primer. Elsevier Academic Press, San Diego.